An Investigation of the Swelling Kinetics of Bentonite Systems Using Particle Size Analysis

Musaab I. Magzoub, Ibnelwaleed A. Hussein, Mustafa S. Nasser, Mohamed Mahmoud, Abdullah S. Sultan & Abdelbaki Benamor

Published online: 14 May 2019.

Submit your article to this journal ☑

Article views: 770

View related articles ☑

View Crossmark data ☑

Taylor & Francis
Taylor & Francis Group

An Investigation of the Swelling Kinetics of Bentonite Systems Using Particle Size Analysis

Musaab I. Magzoub[a], Ibnelwaleed A. Hussein[a] (iD), Mustafa S. Nasser[a] (iD), Mohamed Mahmoud[b], Abdullah S. Sultan[b] (iD), and Abdelbaki Benamor[a]

[a]Gas Processing Center, College of Engineering, Qatar University, Doha, Qatar; [b]Petroleum Engineering Department, College of Petroleum and Geosciences, KFUPM, Dhahran, Saudi Arabia

ABSTRACT

Particles size distribution (PSD) is introduced as a tool for analysis of bentonite aggregation and swelling kinetics. Raw Ca-bentonite was purified using a combined wet sieving and sedimentation processes, followed by thermochemical treatment with Na_2CO_3 to increase its swelling capacity. The detailed analysis of the PSD shows a strong correlation between the PSD and the swelling process. For the chemically treated raw bentonite, PSD revealed two different peaks representing unswelled and swelled particles along with some aggregates. The swelling is shown to be a kinetically controlled process that depends on time, temperature, and bentonite chemical composition. At the beginning of the chemical treatment, the effect of aggregates was more dominant; therefore, the viscosity did not increase much with particle size. However, the combined chemical and thermal treatment has enhanced the Na-activation process and boosted bentonite swelling. The rheological measurements have shown enhancement in the viscosity and confirmed the PSD findings. The same optimal treatment conditions are obtained from both rheological measurements and PSD analysis. A model is developed based on classical reaction rate kinetics and used to describe the conversion from unswelled to swelled particles. The PSD has a strong correlation with the physical properties of the suspension such as the viscosity. The swelling rate fits a second order model with a rate constant, k, in the range 0.002 to $0.124\,h^{-1}$ and an activation energy, E, of 87 kJ/mol. PSD analysis together with the developed kinetic model are powerful tools for studying the swelling kinetics of bentonites.
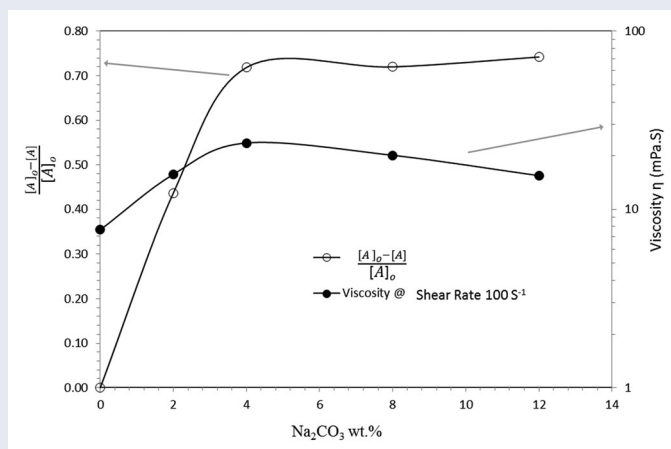
GRAPHICAL ABSTRACT

1. Introduction

The unique ability of bentonite to absorb water and swell many times its dry volume, and its extremely low water permeability, make bentonite an ideal candidate for many industrial and engineering applications. Naturally, bentonite is classified into two types, The Na-bentonite, which has a high swelling capacity, and the Ca-bentonite, which is a non-swelling clay that forms a colloidal suspension in water[1]. The major uses of bentonite are in drilling fluids, paints, paper making, fillers and extenders and in civil

engineering applications[2–10]. Bentonite is used to prepare drilling fluid, a viscous water-based fluid containing all required additives, used in drilling of oil and gas wells. Drilling fluid increases the viscosity and reduces the filtration losses of water to the surrounding rocks of the wellbore, as water is trapped between the bentonite layers[11,12].

Study of the swelling of bentonite is very important for many engineering applications related to drilling fluids, and other uses of bentonite, such as flocculation, soil stabilization, and environmental applications[8,13,14]. Our recent work has shown that swelling has a strong influence on the rheological properties of bentonite [15]. Thus, most of the previous studies use rheological measurements to study bentonite colloidal systems. The rheological behavior of structural 2-phase fluids is directly related to the size of the particles of the dispersed phase, such as in swelled-clay dispersions[16,17]. Viscoelastic properties are related to the network of flocculated particles, and the inter-particle interactions between the colloidal particles[18,19].

Bentonite suspensions fall into the category of solid particles dispersed in a liquid and are considered as structured fluids[20]. Conventionally, the interpretation of many properties of clay suspensions is based on a model which assumes separated clay plates with a well-developed electrical double layer, and a dynamic equilibrium governs the average size of particles in a montmorillonite suspension[21,22]. Such fluids are highly thixotropic and the rheological measurements are often time consuming and challenging due to the disturbance of the microstructure during sample loading[23].

Numerous studies have emphasized the proportional relationship between the swelling and the rheological properties of colloidal systems[24–26]. However, only a very few studies have directly correlated swelling characteristics and viscosity measurements[27,28]. Particle size analysis indicates that the treatment of bentonite with an ionic liquid increases the particle size due to swelling, which increases the viscosity[29]. Naghib et al. (2017) have presented a comparative hydrodynamic analysis of the expansion rate of alginate beads in terms of the swelling characteristics and size distribution, and a comparison of the fluidization properties with the expansion properties[30]. A study by Takahashi and Fujita (2017)[31] of structural mixtures such as starch, indicates that, the swelling and gelatinization process taking place when starch is heated, increase concurrently with increasing heating temperature. In addition, the viscoelastic properties are governed by the volume fraction of the particles that are not ruptured during heating. For example, rheological properties of cellulosic slurries are influenced by the particle size and the rate of the hydrolysis reaction, indicated by a drop in the viscosity due to the fragmentation of the cellulose particles[32,33]. Particle size distribution (PSD) was also reported to be used as a method of analysis for the effect of agitation speed and concentration of suspension stabilizer on polymerization of Methyl Methacrylate, and an empirical equations correlating the average particle size and the PSD were derived from the study[34].

Swelling of bentonite and its properties can be enhanced by applying different treatment methods, such as using inorganic additives. Addition of Na_2CO_3 is a well-known method of enhancing the quality of bentonite[35]. The addition of very small amounts of Na_2CO_3 can significantly enhance the properties of bentonite, a method that the industry has used for decades. The sodium content has a large effect on the dispersion characteristics of bentonite. An increase of the Na/Ca ratio considerably enhances the swelling capabilities of bentonite, significantly affecting its physical properties[36,37]. The PSD has a great impact on stability, purification efficiency, swelling, and rheological properties of bentonite suspension[38–40]. Moreover, the results of PSD measurement by dynamic light scattering (DLS) can be linked to the rheology of the suspensions or to the stability of emulsions [41]. Rheology of bentonite suspensions depends on many parameters beside the particle size, such as the concentration, the state of hydration of the bentonite particles, the presence of ions, temperature, and pH of the suspension[42,43].

In this paper, the swelling kinetics of bentonite is investigated using PSD analysis. A laser scattering technique is introduced as a new method for investigating and modeling bentonite swelling kinetics using PSD data. The new method uses known kinetic models that are developed to describe the physical swelling process. Rheological measurements are used to validate and confirm the PSD results.

Theory

The swelling process of bentonite involves the combination of water molecules and bentonite particles forming swelled hydrated particles. The formation of bentonite containing swelled particles, with a large particle size, leads to a positive shift in the PSD. The fractional conversion of swelled particles is defined here as the ratio of the area under the frequency versus PSD curve for swelled particles to the same of the initial PSD of unswelled particles. This conversion from unswelled to swelled particles is a kinetically controlled process, which resembles that of a classical chemical reaction.

Montes-h et al. (2003)[44] have studied the swelling kinetics of bentonite using environmental scanning electron microscopy through direct measurements of swelling. The results indicate a nonlinear swelling behavior and a first order model does not fit the experimental data. Schott (1992)[45] studied the swelling kinetics of thin films of gelatin and developed a theoretical model for the swelling process. The author showed that second order kinetics fit the experimental data for diffusion-controlled swelling rather than first order kinetics. The author has provided a detailed explanation of the second order swelling kinetics and assumed that the rate of swelling is proportional to two quantities. The first quantity is the fractional amount of the swelling capacity (unswelled fraction) and the second quantity is the specific surface envelope that encloses sites that are yet to interact with water (unswelled parts).

Here a kinetic model for bentonite swelling, based on chemical reaction models in which species A (bentonite) and B (water) are converted to C (swelled bentonite) through a reaction, is introduced. The rate of the chemical reaction is determined by the change in concentration of the reacting substances, A and B, to form a product C.

Table 1. EDX analysis for raw, purified and activated bentonite

Element	Commercial Raw Wet Sieved Bentonite	Thermochemically Ca-Bentonite	Bentonite	Treated Bentonite
O	58.5	50.26	52.88	52.82
Na	1.39	1.73	1.77	6.6
Mg	0.9	1.46	1.36	1.42
Al	6.8	9.59	9.49	8.6
Si	28.9	25.1	25.31	22.91
Cl	–	1.22	1.6	2.83
K	0.19	0.54	0.59	0.31
Ca	0.48	0.91	0.89	0.4
Ti		0.83	0.89	0.41
Fe	2.69	6.64	3.83	3.57
Cu	–	0.74	0.57	0.13
Zn	–	0.88	–	–
S	0.15	–	–	–
Na/Ca ratio	2.896	1.91	1.98	16.5

$$aA + bB \rightarrow cC \qquad (1)$$

Assuming that the liquid phase reaction is elementary, the reaction rate (k) is proportional to the reacting species A and B quantitatively as follows[46]:

$$Rate = -\frac{d[A]}{dt} = k_1[A]^a[B]^b \qquad (2)$$

The above equation can be re-written in terms of the concentration of A, [A], as:

$$Rate = -\frac{d[A]}{dt} = k[A]^n \qquad (3)$$

where k is a lumped rate parameter and n is the order of the reaction, which can be determined from the measurement of the concentration of the unswelled particles at any time t and the initial concentration. The area under the curve of the frequency versus the size of unswelled particles initially is considered as the initial concentration, $[A]_o$; the area under the curve in the same initial frequency range at any time, [A], represents the unswelled particles at any time. For a first order reaction, a plot of $\ln\frac{[A]_o}{[A]}$vs t should be linear, and the slope is the rate constant, k. However, for a second order reaction a plot of 1/[A] vs t is linear with a slope k.

For the analysis of PSD, the number average or the first moment (D_n) and the weight average or the second moment (D_w) are used to describe the swelling behavior of bentonite. These parameters are defined as follows:

$$D_n = \sum \left[\frac{N_i \ D_i}{N_i}\right] \qquad (4)$$

$$D_w = \sum \left[\frac{N_i \ D_i^2}{N_i \ D_i}\right] \qquad (5)$$

$$D_z = \sum \left[\frac{N_i \ D_i^3}{N_i \ D_i^2}\right] \qquad (6)$$

where D_i is the particle size with a frequency N_i, $D_n$is the number-average particle size, $D_w$is the weight-average particle size, and D_z is the volume or surface mean, which represents the average size of the particles that occupy a majority of the volume. Usually, $D_w$is located at the peak of the distribution, hence it correlates very well with physical properties of the suspension since it represents the majority of the PSD. The ratio D_w/D_n is the dispersity index (DI) which reflects the breadth of the distribution. If DI is in the range 1-2, the particles are monodispersed.

2. Experimental

2.1. Material

Raw Ca-Bentonite with a low swelling capacity was obtained from a local deposit in Saudi Arabia. The chemical composition of raw bentonite (Table 1) identifies the type of clay as Ca-bentonite[47]. The composition of raw bentonite determined using energy-dispersive X-ray spectroscopy (EDX) is as follows; oxygen (51.19%), silicon (25.1%), aluminum (9.59%), magnesium (1.46%), and potassium (0.54%). The sodium/calcium ratio of raw and purified Ca-bentonite is in the range of 1.91 to 1.98. This Na/Ca ratio is considered to be low and typically results in a low swelling capacity[48].

Sodium carbonate (Na_2CO_3), commonly known as soda ash, was used to treat the raw local bentonite to increase its Na/Ca ratio and hence the swelling capacity. The Na_2CO_3 used was in a pure fine powder form. The treatment was conducted at different temperatures in a wet process by adding Na_2CO_3 to water prior to the addition of bentonite, with stirring. The Na/Ca ratio of the activated bentonite was determined using EDX conducted using a scanning electron microscopic (SEM-EDX, Oxford Instruments) analysis of the treated samples. A Fritsch Particles Size analyzer model ANALYSETTE 22 NanoTec (0.01 – 2100 μm) was used in this study. Rheological measurements were conducted to confirm the swelling of bentonite, which affects the viscosity of swelled bentonite. A concentric cylinder rheometer, from TA Instrument (Model-DHR) was used for the rheological measurements. The concentric cylinder rheometer includes a cup with a radius of 15 mm, and is configured with a DIN rotor with a diameter of 14 mm and height of 42 mm with a maximum heating range of 13 °C/min.

2.2. Methods

2.2.1. Beneficiation of raw bentonite

Raw bentonite contains many clay and non-clay impurities such as sand, quartz, feldspar, iron, and silica. Raw
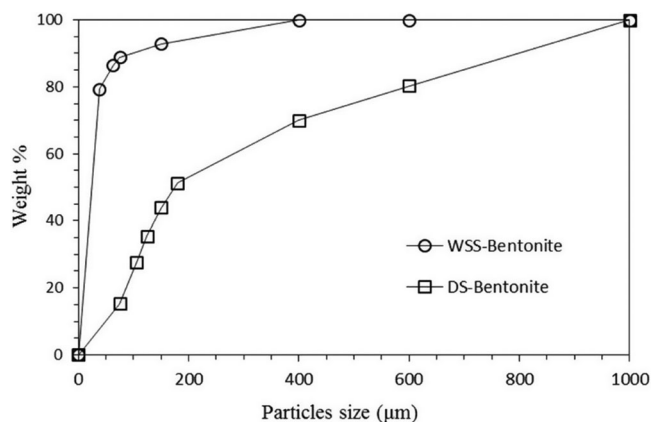
Figure 1. Bentonite recovery from wet and dry sieving.

bentonite has a wide PSD due to the presence of impurities. Beneficiation of bentonite is the purification process, in which the impurities are removed from raw bentonite, either by dry or wet sieving. Stable colloidal suspensions are formed when bentonite is dispersed in water (1:5 by weight) for 24 h. Any sand or quartz impurities will not be suspended and will rapidly settle down during this process. Suspension and sedimentation of the particles in water depends on many factors, such as the particle size, pH, time, concentration, and temperature[49]. Mechanical dry sieving can generate a PSD with a range of sizes (75 μm - 600 μm). Prior to dry sieving, samples were reasonably ground using a milling machine, and dried in an oven for 16 h at 105 °C to remove moisture. For dry sieving, a known weight of the dried bentonite was loaded into the top tray of a sieve shaker. During sieving the particles were retained on sieve trays and fractionated based on their sizes. Sedimentation by wet sieving (75 μm mesh No. 200) yielded a higher recovery of pure bentonite compared to dry sieving (Figure 1).

Figure 1 shows the percent bentonite recovered from the sieves used for dry sieving (DS-Bentonite) and wet sieving after sedimentation (WSS-Bentonite). In dry sieving, as particles are sticking together, the recovery is reduced. Sedimentation disperses the particles and allows pure clay to be easily separated. In wet sieving, grinding of the impurities to a fine powder that can pass through during dry sieving is avoided. Typically, to have a uniform distribution the targeted particle size of commercial bentonite is below 75 μm. Dry sieving resulted in a recovery of 15 wt.%, while wet sieving produced a recovery of more than 80 wt.%. Thus, wet sieving was used in this study.

2.2.2. Treatment to improve swelling
Raw Ca-bentonite was treated with Na_2CO_3 to improve swelling by increasing the Na/Ca ratio to achieve the desired rheological properties[36]. Energy-dispersive X-ray spectroscopy indicates that the Na/Ca ratio of the activated bentonite samples is high. The ratio increased from 2.9 up to 16.5 for the fully activated samples, as shown in Table 1. A 6 wt.% sample of WSS-Bentonite was used for Na_2CO_3 treatment. Na_2CO_3 was added to water before WSS-Bentonite and the mixture was stirred using a high-speed mixer for

5 minutes. After the Na_2CO_3 activation, the samples were subjected to heating while stirring (25 to 65 °C) for a specific time to enhance the Na-activation and the swelling processes. As about 2.5% of water had evaporated at the end of the hot stirring process, deionized water was added to compensate for the evaporation loss and maintain the same bentonite concentration in the suspension. PSD of all samples was measured to develop the swelling kinetics model(s). Rheological measurements were employed to validate and confirm the results of the PSD analysis.

3. Results and Discussion

### 3.1. Beneficiation of bentonite to obtain a uniform PSD
Beneficiation process removes impurities leaving only the bentonite particles with a more uniform size distribution (as shown in Figure 2a) with 90% of the particles of less than 10 μm (Figure 2b). Raw bentonite has a broad distribution of particle sizes ranging from 0.8 μm to 2000 μm. Sedimentation and wet sieving through 75 μm remove impurities of larger particles such as iron and non-clay content (Table 1), making the PSD narrower and uniform as determined from the PSD curve, matching that of the commercially available bentonite, (Figure 2a).

3.2. Effect of chemical treatment at 25 °C on PSD and rheology
Suspension of bentonite in water leads to the swelling of bentonite platelets due to the ingress of water molecules. PSD was determined after aging for 24 hours to allow the full hydration of 6 wt.% wet-sieved bentonite (WSS-Bentonite) both before chemical treatment (i.e., Ca-bentonite) and after Na_2CO_3 activation (i.e., Na-bentonite). Aging of the bentonite suspension allows full hydration, and improves the properties of bentonite in water[50]. The results in Figure 3a show that the untreated Ca-bentonite does not have adequate swelling capacity indicated by the single narrow peak in the PSD plot (around 2.4 μm). After the activation with Na_2CO_3 (2 to 12 wt.%), the PSD plot was altered, showing two peaks, as depicted in Figure 3b-e. Particles have swelled to a certain extent with the addition of Na_2CO_3, while some of the particles remained unswelled, resembling the original peak in the same range of particles sizes, i.e., 2.4 to 5 μm (Figure 3 b-e).

The appearance of the two peaks in the PSD plot reflects that the conversion of unswelled bentonite to swelled bentonite (as described by equations 4-6 above) is not complete. Therefore, only a fraction of the particles in raw bentonite is converted (combined with water) to larger particles. The first peak has an average size of ~5 μm representing the untreated portion of the particles. The second peak has an average size of ~1000 μm representing the swelled particles. The initial average particle size of 2.4 μm increased to more than 1000 μm with chemical treatment. When the Na_2CO_3 concentration was increased above 4 wt.%, the particle size did not increase anymore above the maximum average
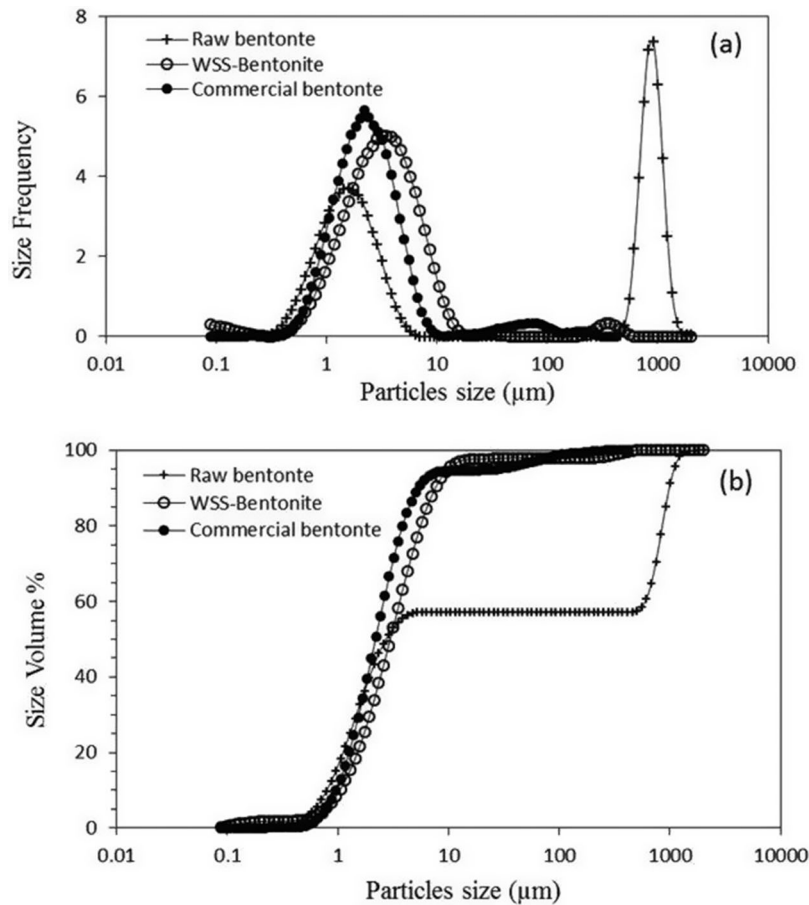
Figure 2. Effect of purification of raw bentonite on the PSD compared to commercial bentonite.

particle size of 1287 μm. The results indicate that the chemical treatment significantly improves the swelling of bentonite.

The PSD of bentonite activated with Na_2CO_3 (Na-bentonite) was analyzed using statistical methods to calculate the first, second, and third moments and the values of D_n, D_w, and D_z described by equations 4-6 were calculated and are shown in Table 2. These results were obtained from the PSD analysis of samples aged for 24 h to achieve the maximum possible hydration of the treated bentonite at room temperature. The results indicate that treating bentonite with more than 4 wt.% of Na_2CO_3 does not affect the values of D_n, D_w and D_z. In addition, the values of unswelled particles, [A], remain almost constant for bentonite samples treated with 4 wt.% Na_2CO_3 or more. However, the addition of more Na_2CO_3 to the unswelled particles leads to a more uniform PSD as indicated by the lower values of the dispersity index, DI. Addition of very high amounts of Na_2CO_3, as high as 12%, results in a drop in D_z, which suggests that the number of particles with larger sizes in the distribution (highly swelled particles) is decreasing (D_z is strongly influenced by larger particles than small ones).

The area under the PSD plot was calculated to estimate the fraction of particles that does not swell by the chemical treatment, and the values are given in Table 2. The area under the PSD plot indicates that the initial peak $[A]_o$ decreases with increasing Na_2CO_3 and the unswelled fraction, $[A]/[A]_o$, also decreases. Thus, the size of the particles is increasing, which is manifested by a second peak appearing at higher values of particle size. The calculated area under the curve, $([A]_o-[A]/[A]_o)$, which represents the swelled fraction of raw bentonite, was plotted against the concentration of Na_2CO_3 added in each step (see Figure 4).

Above 4 wt.%, further significant swelling does not occur. Thus, the PSD results suggest that wt.% of Na_2CO_3 is the optimal amount for treating bentonite. The results of the PSD measurements are supported by the results of the rheological measurements (shown in Figure 4). The viscosity increases with increasing Na_2CO_3 content, reaching a maximum at 4% and then decreased, which is in agreement with the findings of the PSD measurements. The values of viscosity at a shear rate of $100 \, s^{-1}$ was selected for validation to mimic drilling fluid operating conditions. However, the trend is valid for all shear viscosity values as shown in our previous work (Magzoub et al. (2018) Figs. 2&3)[15]. The addition of large amounts of Na_2CO_3 decreases the viscosity, which is likely due to a drop in the number of large particles, i.e. a decrease of D_z and DI, which is in agreement with the results shown in Table 2. These observations are in agreement with our earlier work on emulsions, where the droplet size was shown to influence the rheology[51]. Hence, the rheology measurements support and validate the findings of the PSD analysis.
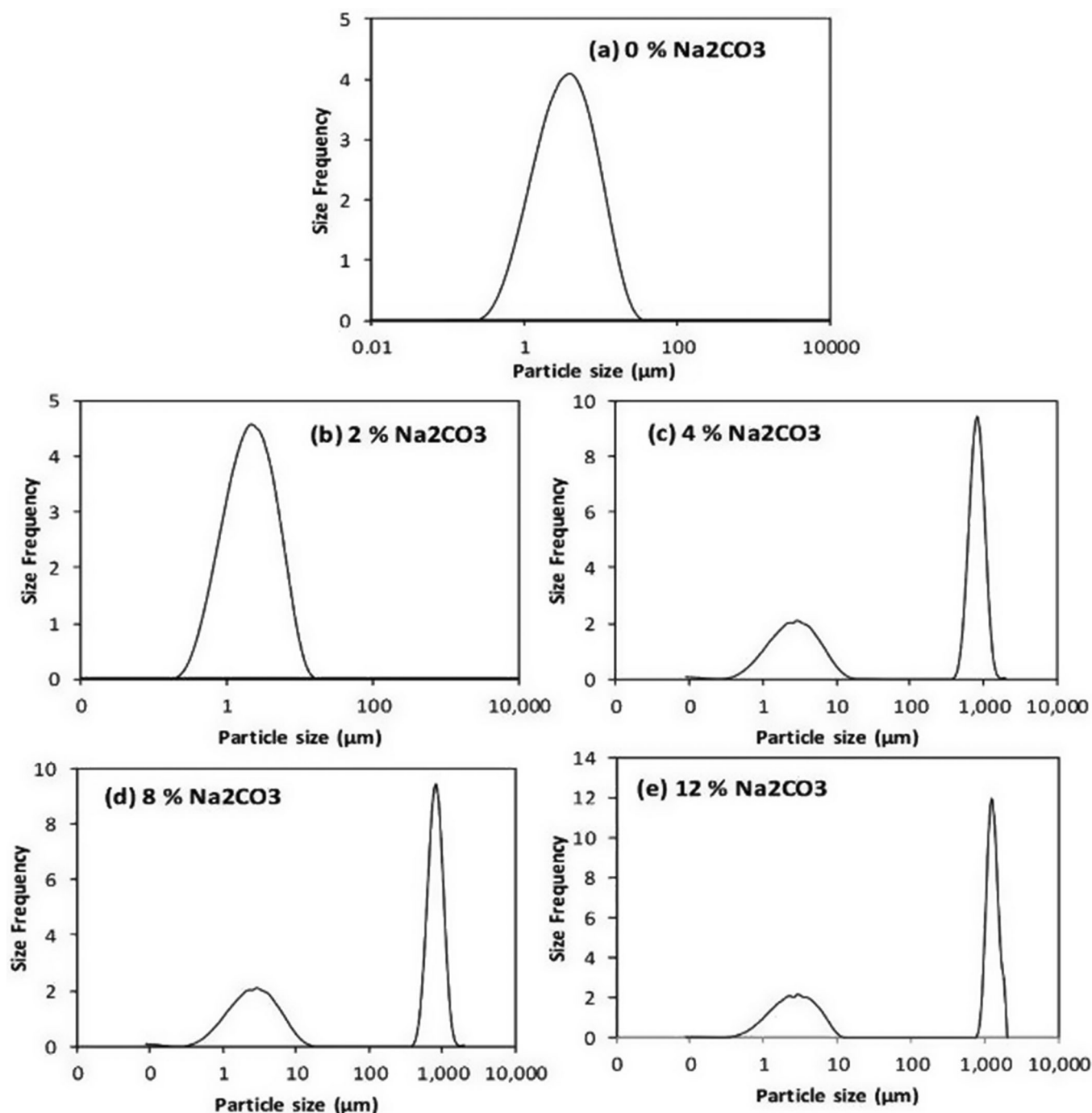
Figure 3. Effect of the Na_2CO_3 treatment on swelling using PSD.

3.3. Effect of thermal treatment on the PSD of bentonite

After 24 hours of soaking at room temperature, Ca-bentonite did not show any swelling. However, when Na-bentonite is used, about 70% of the particles are converted to swelled particles during the same period ($[A]_o=49$ and $[A]_o-[A]=35.5$). The process was repeated for Na-bentonite at higher temperatures using the optimal amount of Na_2CO_3 of 4 wt.% and the PSD and rheology measurements were conducted. The process of chemical treatment with Na_2CO_3 combined with heating and stirring is expected to improve the swelling of bentonite[52]. Thermal treatment greatly improves the rheological properties, indicated by the

Table 2. Impact of Na2CO3 addition at room temperature on PSD analysis after 24 hrs.

Na_2CO_3 wt.%	[A]	$[A]/[A]_o$	1/[A]	D_n	D_w	D_z	DI
0%	49.46	1.00	0.02	4.97	9.06	13.38	1.82
2%	27.86	0.56	0.04	2.80	4.62	6.69	1.65
4%	13.92	0.28	0.07	3.31	5.24	7.53	1.58
8%	13.86	0.28	0.07	3.31	5.24	7.53	1.58
12%	12.76	0.26	0.08	3.08	4.48	5.73	1.45

increase of the viscosity with heating and stirring. The particles undergo thermal expansion and heat will improve the water diffusion between the bentonite platelets. The swelling capacity increases significantly when Na-activation is
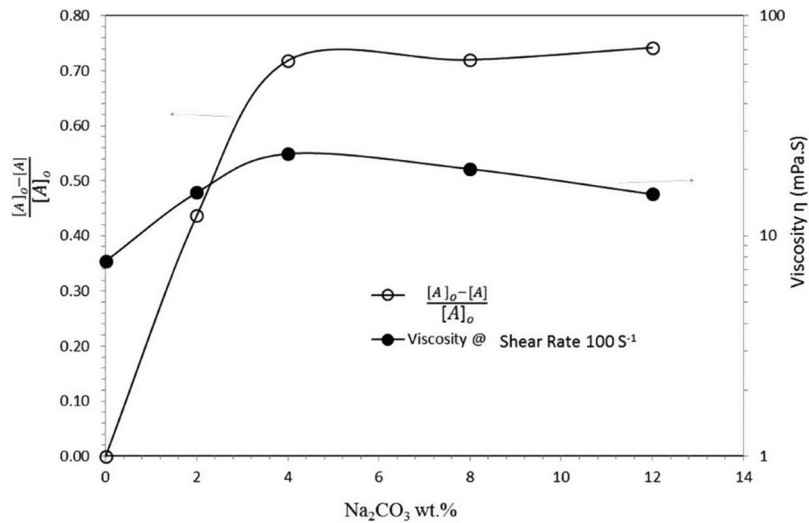
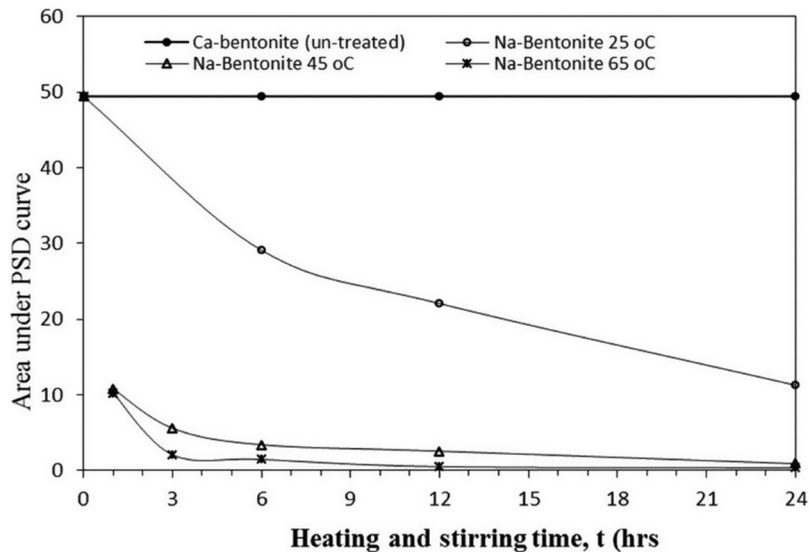**Figure 4.** The effect of Na$_2$CO$_3$ treatment on swelling and rheology.

Figure 5. Effect of combined heating and stirring on PSD of Ca-bentonite and Na-bentonite.

combined with heating and stirring at 25 °C, 45 °C, and 65 °C. As shown in Figure 5, the area under the first peak of the PSD plot, which is due to the unswelled particles, decreases with increasing temperature. The unswelled fraction of the particles at any given time, [A]/[A]$_o$, and the statistical analysis of PSD are given in Table 3. At 65 °C and after 24 h, the concentration [A] is almost zero (A$_o$-A = 0.35 which represents less than 1% of [A]$_o$) as shown in Table 3. Under these conditions, the first peak almost disappears as the swelled fraction of the particles (the second peak) increases with temperature, as depicted in Figure 6. The average particle size increases from 2.4 μm for untreated bentonite to 1287 μm. In addition, the values of DI and D$_Z$ decrease with time suggesting the presence of a uniform distribution. These results on bentonite are in agreement with the work of Takahashi and Fujita (2017) [31] on starch.

Heating time is crucial to speed-up the swelling process of bentonite. For economic reasons, the determination of the optimal heating time is important. PSD analysis was used to obtain the time required to achieve maximum
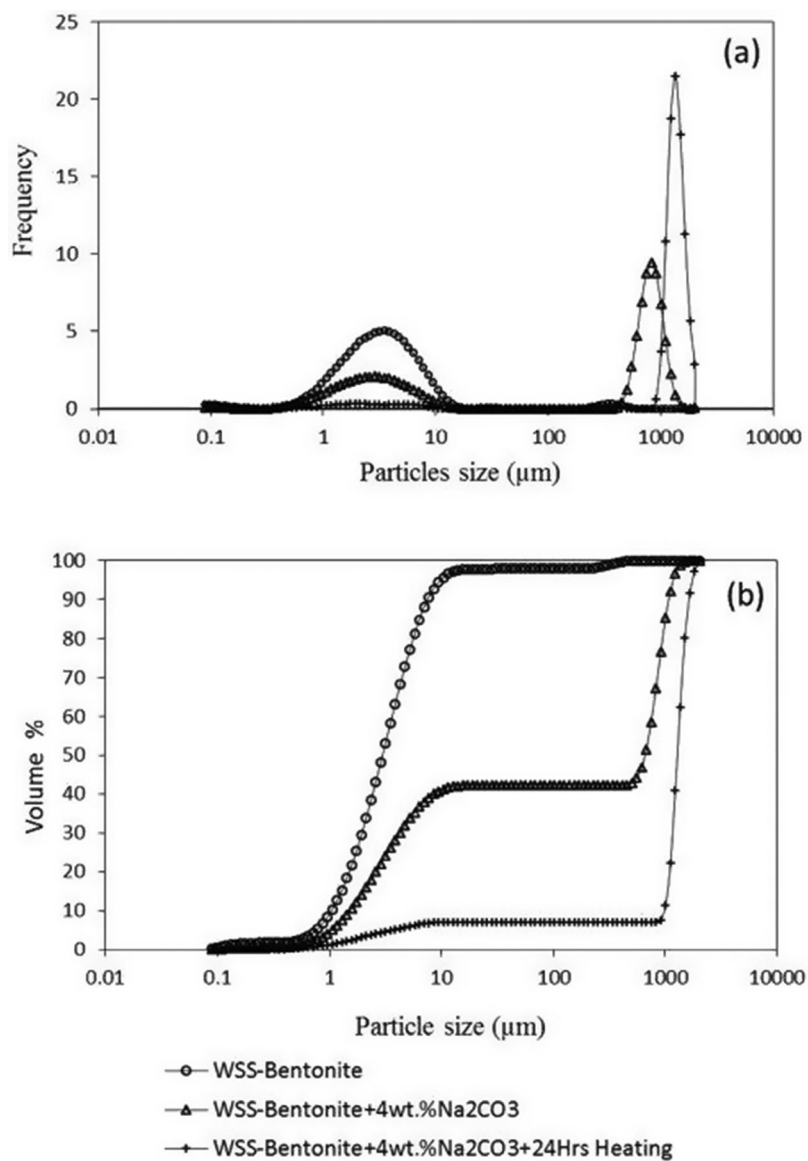
swelling. Ca-bentonite samples were treated with the 4 wt.% Na$_2$CO$_3$, followed by heating/stirring at the 65 °C. The PSD was determined at heating times ranging from 1 to 24 h. Figure 7 shows the values of weight percentage at the index values of D$_{10}$, D$_{50}$, and D$_{90}$. The optimal time of heating/stirring treatment is 3 h, at which all indices reach a maximum and then become constant. Again, the rheological measurements, shown in Figure 7, are used to confirm the results of PSD analysis.

The heat treatment with stirring accelerates the conversion of raw bentonite into swelled bentonite. Thus, heat accelerates the swelling of bentonite suspensions, which is indicated by the results of the PSD and rheological measurements. These results indicate that the swelling of bentonite is a kinetically controlled process. The effect of temperature on the swelling process is shown in Figure 5. In addition, Figure 7 shows that viscosity has significantly increased during the heating period, reaching a flat plateau at 6 h of heating. Thus, the results of the rheology measurements confirm the results of the PSD analysis.

Table 3. Impact of 4 wt.% Na2CO3 on PSD analysis

Treatment @ 25°C

Time (hrs.)	[A]	[A]/[A]$_o$	1/[A]	D_n	D_w	D_z	DI
0	49.46	1	0.0202	4.9691	9.05743	13.378	1.8228
6	29.11	0.588	0.0344	4.98629	9.42386	14.272	1.89
12	22.1	0.447	0.0452	3.58815	6.06085	10.295	1.6891
24	11.3	0.228	0.0885	1.33359	2.16406	2.8693	1.6227

Treatment @ 45°C

Time (Hrs.)	[A]	[A]/[A]$_o$	1/[A]	D_n	D_w	D_z	DI
0	49.46	1	0.0202	4.9691	9.05743	13.378	1.8228
1	10.84	0.219	0.0923	1.08873	1.78331	2.5199	1.638
3	5.602	0.113	0.1785	0.92261	1.67201	2.6943	1.8123
6	3.422	0.069	0.2922	0.54863	0.69374	0.8486	1.2645
12	2.568	0.052	0.3894	0.81264	0.96998	1.133	1.1936
24	0.912	0.018	1.0968	0.56282	0.5952	0.6284	1.0575

Treatment @ 65°C

Time (Hrs.)	[A]	[A]/[A]$_o$	1/[A]	D_n	D_w	D_z	DI
0	49.46	1	0.020	4.969	9.057	13.378	1.823
1	10.28	0.207	0.097	5.360	6.523	11.633	2.048
3	2.10	0.0424	0.477	2.999	4.592	5.833	1.531
6	1.47	0.029	0.679	1.078	1.405	1.615	1.302
12	0.53	0.010	1.901	0.818	1.089	1.198	1.332
24	0.35	0.007	2.825	0.839	1.101	1.199	1.313

—○— WSS-Bentonite

—▲— WSS-Bentonite+4wt.%Na2CO3

—+— WSS-Bentonite+4wt.%Na2CO3+24Hrs Heating

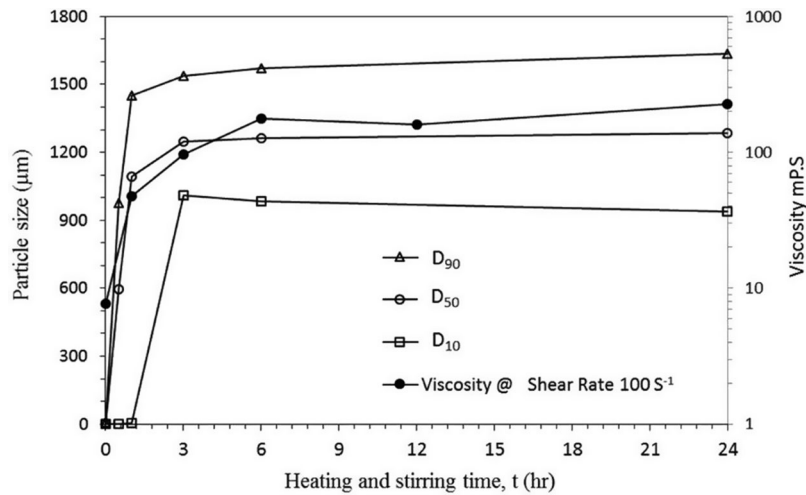**Figure 6.** Effect of the thermochemical treatment on the swelling of bentonite using PSD.

Figure 7. Effect of the heating time on swelling using particles size D_{10}, D_{50}, and D_{90}, and rheology of thermally treated Na-bentonite.
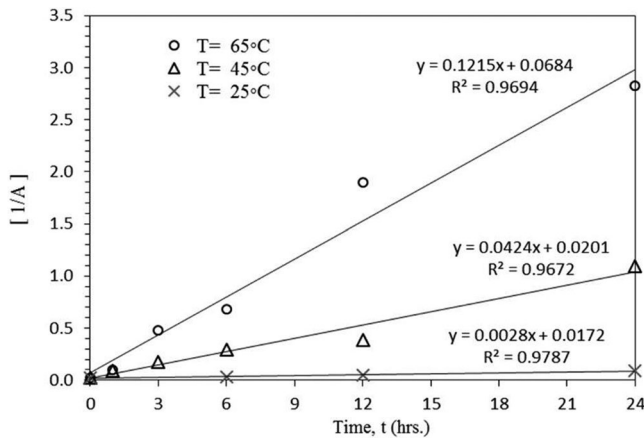

Figure 8. A plot of 1/[A] vs. time for thermally treated Na-bentonite at 25 °C, 45 °C, and 65 °C.

Table 4. Temperature dependence and reaction energy calculation

Temp., °C	Temp., K	k, hr^{-1}	1/T, K^{-1}	ln k
25	298.15	0.002	0.00335	−6.21461
45	318.15	0.042	0.00314	−3.17009
65	338.15	0.124	0.00296	−2.08747
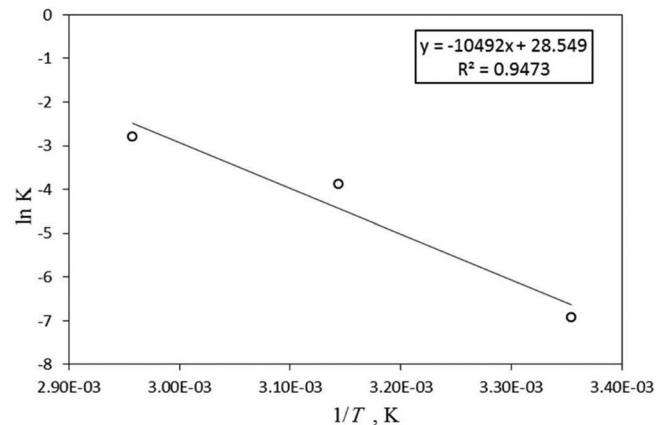
Figure 9. A plot of ln k vs. 1/T, K^{-1} for thermally treated Na-bentonite.

3.4. Modeling of bentonite swelling kinetics using PSD analysis

The results described in the previous section indicate that the swelling of bentonite is a kinetically controlled process that is influenced by both temperature and time. Typically, bentonite suspensions show very pronounced time-dependent behavior, where the yield stress increases significantly with time of aging[53]. In addition, the thermal treatment converts Ca-bentonite to Na-bentonite, improving the swelling behavior. Hence, the swelling process can be viewed, as discussed in the introduction, as an interaction between bentonite and water molecules to form swelled bentonite (see equations 1-3). Thus, classical kinetic rate models seem to be the most suitable for modelling the swelling process. The concept of the proposed model is similar to that of Schott[45]. In both models the swelling rate follows second order kinetics despite the differences in the development of the two models. In addition, the model proposed in this paper uses PSD data while Schott model used direct swelling measurements. The PSD was determined at 3 different temperatures namely 25 °C, 45 °C, and 65 °C. The area under the PSD plot calculated at each temperature as a function of time, [A], is the concentration of unswelled particles at any

time. The total area under the PSD plot for raw bentonite is represented by [A]$_o$.

A plot of ln [A]$_o$/[A] versus t is not linear, indicating that the process does not follow first order kinetics. However, a plot of 1/[A] versus t is linear with a high regression coefficient (R^2=0.97-0.98). The regression coefficient for the first order model is much lower (~R^2=0.665, plots are not shown here). Thus, the second order kinetics were used to model the bentonite swelling process and the results are in agreement with those reported previously[44,45]. The Plot of 1/[A] versus time is shown in Figure 8 and the values of k are calculated from the slope and are given in Table 4. The applicability of second order kinetics rather than first order swelling kinetics for the modeling of the swelling behavior of bentonite suggests that the swelling process is controlled by the diffusion of water between the bentonite layers [34]. The current work, which used PSD analysis, supports the previous work on bentonite swelling

kinetics performed using environmental SEM techniques[44,45].

The rate constant k is defined as k = k_o exp (-E/RT), where k_o is the shape factor, E is the activation energy, R is the universal gas constant, and T is the absolute temperature. A plot of ln k vs 1/T, which is linear with a slope of (-E/RT) as shown by equation 7, can be used to calculate the activation energy:

$$\ln k = k_o - \frac{E}{RT} \tag{7}$$

where E is the activation energy in (J/mol), T is temperature in kelvin, and R is the ideal gas constant (8.314 J/mol K). Figure 9 shows the plot of ln k vs 1/T (K) and the slope is calculated and provided in Table 4. The value of E, obtained from the slope (-E/RT= -10,492 J/mol K), is 87 kJ/mol.

4. Conclusions

In this paper, particle size analysis is introduced, for the first time, as a powerful tool for the analysis of swelling kinetics. Purification of bentonite and a uniform particles size distribution are important to obtain good dispersion properties. EDX shows that the activation of Ca-bentonite with Na_2CO_3 and the thermal treatment increase the Na:Ca ratio. A high Na/Ca ratio enhances the swelling capacity of bentonite. The PSD results are confirmed by independent rheological measurements. The optimal concentration of Na_2CO_3 and the optimal heating time determined by both techniques are 4 wt.% and 3 Hrs., respectively. The increase in particle size is attributed to two mechanisms, the aggregation that took place at the beginning of the chemical treatment and the later swelling due to the expansion of bentonite platelet because of sodium activation. The swelling process is a kinetically controlled process that depends on time, temperature, and composition of bentonite, especially the Na/Ca ratio. Therefore, the proposed thermochemical Na-activation has enhanced the process of conversion of unswelled particles to swelled particles. The increase and decrease in the viscosity with the amount of Na_2CO_3 used to treat bentonite is explained and correlated with the PSD, especially D_w and the dispersity index. In addition, Na_2CO_3 treatment combined with heating and stirring greatly enhance the swelling capacity of bentonite. In agreement with previous literature reports[44,45], the swelling process follows second order kinetics with a rate constant, k, in the range 0.002 to 0.124 hr^{-1} and an activation energy, E, of 87 kJ/mol. The applicability of second order swelling kinetics rather than first order swelling kinetics to explain the bentonite swelling behavior suggests that the swelling is a diffusion-controlled process [34]. The proposed model shows that particle size analysis can be used for studying the swelling kinetics of bentonites and could be extended for studying other swelling systems for a range of engineering applications.

ORCID

Ibnelwaleed A. Hussein http://orcid.org/0000-0002-6672-8649
Mustafa S. Nasser http://orcid.org/0000-0002-7646-558X
Abdullah S. Sultan http://orcid.org/0000-0001-9617-4678

References

[1] Hassan, M.; Abdel-Khalek, N. Beneficiation and applications of an Egyptian bentonite. Applied Clay Science 1998, 13, 99–115. DOI: 10.1016/S0169-1317(98)00021-0.

[2] Eisenhour, D.D.; Brown, R.K. Bentonite and its impact on modern life. Elements 2009, 5, 83–88. DOI: 10.2113/gselements.5.2.83.

[3] Boki, K.; Kubo, M.; Wada, T.; Tamura, T. Bleaching of alkali-refined vegetable oils with clay minerals. Journal of the American Oil Chemists Society 1992, 69, 232–236. DOI: 10.1007/BF02635892.

[4] Christidis, G.E.; Kosiari, S. Decolorization of vegetable oils: a study of the mechanism of adsorption of B-carotene by an acid-activated bentonite from Cyprus. Clays and Clay Minerals 2003, 51, 327–333 DOI: 10.1346/CCMN.2003.0510309..

[5] Makhoukhi, B.; Didi, M.; Villemin, D.; Azzouz, A. Acid activation of Bentonite for use as a vegetable oil bleaching agent. Grasas y aceites 2009, 60, 343–349. DOI: 10.3989/gya.108408.

[6] Bixler, H.J.; Peats, S. Paper making. Washington, DC: U.S. Patent and Trademark Office 1993, U.S. Patent No. 5,178,730.

[7] Lorz, R.; Linhart, F.; Auhorn, W.; Matz, M. Production of paper and cardboard. Washington, DC: U.S. Patent and Trademark Office, 1988, U.S. Patent No. 4,749,444.

[8] Shaikh, S.M.; Nasser, M.; Hussein, I.A.; Benamor, A. Investigation of the effect of polyelectrolyte structure and type on the electrokinetics and flocculation behavior of bentonite dispersions. Chemical Engineering Journal 2017, 311, 265–276. DOI: 10.1016/j.cej.2016.11.098.

[9] Jiuyi, Y. Study on Preparation of Flocculant from Bentonite Used in Treatment of Paper-making WasteWater [J]. Non-metallic Mines 2004, 1, 016.

[10] Öncü-Kaya, E.M.; Şide, N.; Gök, Ö.; Özcan, A.S.; Özcan, A. Evaluation on dye removal capability of didodecyldimethylammonium-bentonite from aqueous solutions. Journal of Dispersion Science and Technology 2017, 38, 1211–1220. DOI: 10.1080/01932691.2016.1229199.

[11] Gidal, B.; Maly, M.; Budde, J.; Lensmeyer, G.; Pitterle, M.; Jones, J.; Caenn, R.; Chillingar, G. Drilling fluids: state of the art. Journal of Petroleum Science and Engineering 1996, 14, 221–230. DOI: 10.1016/0920-4105(95)00051-8.

[12] Barnes, H.A. A review of the slip (wall depletion) of polymer solutions, emulsions and particle suspensions in viscometers: its cause, character, and cure. Journal of Non-Newtonian Fluid Mechanics 1995, 56, 221–251. DOI: 10.1016/0377-0257(94)01282-M.

[13] Alandis, N.; Aldayel, O.; Mekhemer, W.; Hefne, J.; Jokhab, H. Thermodynamic and kinetic studies for the adsorption of Fe (III) and Ni (II) ions from aqueous solution using natural bentonite. Journal of Dispersion Science and Technology 2010, 31, 1526–1534. DOI: 10.1080/01932690903294097.

[14] El-Mallah, N.M.; Hassouba, H.M. Kinetic and Thermodynamic Studies for the Removal of Nickel Ions from an Aqueous Solution by Adsorption Technique. Journal of Dispersion Science and Technology 2014, 35, 130–142. DOI: 10.1080/01932691.2013.769173.

[15] Magzoub, M.I.; Nasser, M.S.; Hussein, I.A.; Benamor, A.; Onaizi, S.A.; Sultan, A.S.; Mahmoud, M.A. Effects of sodium carbonate addition, heat and agitation on swelling and rheological behavior of Ca-bentonite colloidal dispersions. Applied Clay Science 2017, 147, 176–183. DOI: 10.1016/j.clay.2017.07.032.

[16] Agha, M.A.; Ferrell, R.E.; Hart, G.F.; El Ghar, M.S.A.; Abdel-Motelib, A. Physical properties and Na-activation of Egyptian bentonitic clays for appraisal of industrial applications. Applied Clay Science 2015, 131, 74–83. DOI: 10.1016/j.clay.2015.08.016.

[17] Barast, G.; Razakamanantsoa, A.-R.; Djeran-Maigre, I.; Nicholson, T.; Williams, D. Swelling properties of natural and modified bentonites by rheological description. Applied Clay Science 2016, 142, 60–68. DOI: 10.1016/j.clay.2016.01.008.

[18] Tadros, T.F. Correlation of viscoelastic properties of stable and flocculated suspensions with their interparticle interactions. Advances in colloid and interface science 1996, 68, 97–200. DOI: 10.1016/S0001-8686(96)90047-0.

[19] Johnson, S.B.; Franks, G.V.; Scales, P.J.; Boger, D.V.; Healy, T.W. Surface chemistry–rheology relationships in concentrated mineral suspensions. International Journal of Mineral Processing 2000, 58, 267–304. DOI: 10.1016/S0301-7516(99)00041-1.

[20] Luckham, P.F.; Rossi, S. The colloidal and rheological properties of bentonite suspensions. Advances in colloid and interface science 1999, 82, 43–92. DOI: 10.1016/S0001-8686(99)00005-6.

[21] Schramm, L.L.; Kwak, J.C. Influence of exchangeable cation composition on the size and shape of montmorillonite particles in dilute suspension. Clays and Clay Minerals. 1982, 30, 40. DOI: 10.1346/CCMN.1982.0300105.

[22] Maxim, L.D.; Niebo, R.; McConnell, E.E. Bentonite toxicology and epidemiology–a review. Inhalation toxicology 2016, 28, 591–617. DOI: 10.1080/08958378.2016.1240727.

[23] Stokes, J.; Telford, J. Measuring the yield behaviour of structured fluids. Journal of Non-Newtonian Fluid Mechanics 2004, 124, 137–146. DOI: 10.1016/j.jnnfm.2004.09.001.

[24] Farrokhpay, S.; Ndlovu, B.; Bradshaw, D. Behaviour of swelling clays versus non-swelling clays in flotation. Minerals Engineering 2016.

[25] Yao, Z.; Grishkewich, N.; Tam, K. Swelling and shear viscosity of stimuli-responsive colloidal systems. Soft Matter 2013, 9, 5319–5335. DOI: 10.1039/c3sm50374g.

[26] Philippe, A.; Baravian, C.; Bezuglyy, V.; Angilella, J.; Meneau, F.; Bihannic, I.; Michot, L. Rheological study of two-dimensional very anisometric colloidal particle suspensions: from shear-induced orientation to viscous dissipation. Langmuir 2013, 29, 5315–5324. DOI: 10.1021/la400111w.

[27] Zhu, W.; Lou, Y.; Liu, Q.; Song, H.; Wang, J.; Yue, M. Rheological Modeling of Dispersion System of Nano/Microsized Polymer Particles Considering Swelling Behavior. Journal of Dispersion Science and Technology 2016, 37, 407–414. DOI: 10.1080/01932691.2015.1038348.

[28] Mu, Y.; Zhao, G.; Chen, A.; Wu, X. Modeling and simulation of three-dimensional extrusion swelling of viscoelastic fluids with PTT, Giesekus and FENE-P constitutive models. International Journal for Numerical Methods in Fluids 2013, 72, 846–863. DOI: 10.1002/fld.3760.

[29] Nasser, M.; Onaizi, S.A.; Hussein, I.; Saad, M.; Al-Marri, M.; Benamor, A. Intercalation of ionic liquids into bentonite: Swelling and rheological behaviors. Colloids and Surfaces A: Physicochemical and Engineering Aspects 2016, 507, 141–151. DOI: 10.1016/j.colsurfa.2016.08.006.

[30] Naghib, S.D.; Pandolfi, V.; Pereira, U.; Girimonte, R.; Curcio, E.; Di Maio, F.P.; Legallais, C.; Di Renzo, A. Expansion properties of alginate beads as cell carrier in the fluidized bed bioartificial liver. Powder Technology 2017, 316, 711–717. DOI: 10.1016/j.powtec.2016.12.047.

[31] Takahashi, T.; Fujita, N. Thermal and rheological characteristics of mutant rice starches with widespread variation of amylose content and amylopectin structure. Food Hydrocolloids 2017, 62, 83–93. DOI: 10.1016/j.foodhyd.2016.06.022.

[32] Merlet-Lacroix, N.; Di Cola, E.; Cloitre, M. Swelling and rheology of thermoresponsive gradient copolymer micelles. Soft Matter 2010, 6, 984–993. DOI: 10.1039/b918854a.

[33] Dasari, R.K.; Berson, R.E. The effect of particle size on hydrolysis reaction rates and rheological properties in cellulosic slurries. Applied Biochemistry and Biotechnology 2007, 137, 289–299. DOI: 10.1007/s12010-007-9059-x.

[34] Abu-Ayana, Y.M.; Mohsen, R.M. Study of some variables affecting particle size and particle size distribution of suspension polymerization of methyl methacrylate. Polymer-Plastics Technology and Engineering 2005, 44, 1503–1522. DOI: 10.1080/03602550500207709.

[35] Karagüzel, C.; Çetinel, T.; Boylu, F.; Çinku, K.; Çelik, M. Activation of (Na, Ca)-bentonites with soda and MgO and their utilization as drilling mud. Applied Clay Science 2010, 48, 398–404. DOI: 10.1016/j.clay.2010.01.013.

[36] Lebedenko, F.; Plée, D. Some considerations on the ageing of Na2CO3-activated bentonites. Applied Clay Science 1988, 3, 1–10. DOI: 10.1016/0169-1317(88)90002-6.

[37] Liu, D.; Edraki, M.; Berry, L. Investigating the settling behaviour of saline tailing suspensions using kaolinite, bentonite, and illite clay minerals. Powder Technology 2018, 326, 228–236. DOI: 10.1016/j.powtec.2017.11.070.

[38] Magzoub, M.; Mahmoud, M.; Nasser, M.; Hussein, I.; Elkatatny, S.; Sultan, A. Thermochemical Upgrading of Calcium Bentonite for Drilling Fluid Applications. Journal of Energy Resources Technology 2019, 141, 042902. DOI: 10.1115/1.4041843.

[39] Geng, W. Assessing the Performance of Polymer-Bentonite Mixtures for Hydraulic Barrier Applications. The University of Wisconsin-Madison, 2018.

[40] Zhang, Z.; Ye, W.-M.; Liu, Z.-R.; Chen, B.; Cui, Y.-J. Influences of PSD curve and vibration on the packing dry density of crushed bentonite pellet mixtures. Construction and Building Materials 2018, 185, 246–255. DOI: 10.1016/j.conbuildmat.2018.07.096.

[41] Lin, M.; Chu, F.; Bourgeat-Lami, E.; Guyot, A. Particle size in emmulsion polymerization of octamethyltetrasiloxane. Journal of Dispersion Science and Technology 2005, 25, 827–835. DOI: 10.1081/DIS-200035676.

[42] Kelessidis, V.; Maglione, R. Modeling rheological behavior of bentonite suspensions as Casson and Robertson–Stiff fluids using Newtonian and true shear rates in Couette viscometry. Powder Technology 2006, 168, 134–147. DOI: 10.1016/j.powtec.2006.07.011.

[43] Razi, M.M.; Razi, F.M. An experimental study of influence of salt concentration, mixing time, and pH on the rheological properties of pre-hydrated bentonite slurries treated by polymers. Journal of Dispersion Science and Technology 2013, 34, 764–770. DOI: 10.1080/01932691.2012.695942.

[44] Montes-h, G.; Duplay, J.; Martinez, L.; Mendoza, C. Swelling–shrinkage kinetics of MX80 bentonite. Applied Clay Science 2003, 22, 279–293. DOI: 10.1016/S0169-1317(03)00120-0.

[45] Schott, H. Swelling kinetics of polymers. Journal of Macromolecular Science, Part B: Physics 1992, 31, 1–9. DOI: 10.1080/00222349208215453.

[46] Fogler, H.S. Elements of chemical reaction engineering. 1999.

[47] Hauser, E.A. Colloid science of montmorillonites and bentonites. Clays and Clay Minerals 1953, 2, 439–461. DOI: 10.1346/CCMN.1953.0020136.

[48] Brandenburg, U.; Lagaly, G. Rheological properties of sodium montmorillonite dispersions. Applied Clay Science 1988, 3, 263–279. DOI: 10.1016/0169-1317(88)90033-6.

[49] García-García, S.; Jonsson, M.; Wold, S. Temperature effect on the stability of bentonite colloids in water. Journal of Colloid and Interface Science 2006, 298, 694–705. DOI: 10.1016/j.jcis.2006.01.018.

[50] Abu-Jdayil, B. Rheology of sodium and calcium bentonite–water dispersions: Effect of electrolytes and aging time. International Journal of Mineral Processing 2011, 98, 208–213. DOI: 10.1016/j.minpro.2011.01.001.

[51] Al-Yaari, M.; Hussein, I.A.; Al-Sarkhi, A. Pressure drop reduction of stable water-in-oil emulsions using organoclays. Applied Clay Science 2014, 95, 303–309. DOI: 10.1016/j.clay.2014.04.029.

[52] Magzoub, M.I.; Nasser, M.S.; Hussein, I.A.; Mahmoud, M.A.N.E.; Sultan, A.S. Method of producing sodium bentonite. Washington, DC: U.S. Patent and Trademark Office 2017, U.S. Patent No. 9,676,669.

[53] Lee, C.E.; Chandra, S.; Leong, Y.-K. Structural recovery behaviour of kaolin, bentonite and K-montmorillonite slurries. Powder Technology 2012, 223, 105–109. DOI: 10.1016/j.powtec.2011.07.001.